ADVANCED MATERIALS

DOI: 10.1002/adma.200800530

Aqueous Near-Infrared Fluorescent Composites Based on Apoferritin-Encapsulated PbS Quantum Dots**

By *Barbara Hennequin, Lyudmila Turyanska, Teresa Ben, Ana M. Beltrán, Sergio I. Molina, Mei Li, Stephen Mann, Amalia Patanè,** and *Neil R. Thomas**

The potential of colloidal semiconductor nanocrystals (quantum dots, QDs) to overcome problems encountered by organic fluorophores, such as photobleaching, make them promising candidates as fluorescent labels in biological and medical studies.[1] For use in vivo and deep-tissue imaging, QDs should emit in the near-infrared (NIR) wavelength region of the electromagnetic spectrum where the absorption of biological media, fluorescence of natural fluorophores such as haemoglobin, and light scattering are minimal.[2] They should also be water-soluble, chemically stable, not interfere with biochemical processes and be passively or actively transported across cell membranes. In the last two decades, research on biocompatible QDs has focused on the synthesis and surface modification of Group II-VI semiconductor nanocrystals, such as CdSe.[1,3] These QDs are generally prepared at high temperature in nonpolar organic solvents with phosphine ligands[3] and their solubilization in aqueous solution requires either the use of a second amphipathic molecule that creates a more polar surface on the exterior of the dot or the replacement of the coating ligand by a more hydrophilic ligand such as lipoic acid. Furthermore, conjugation of peptide/oligosaccharide tags to these nanocrystals requires them to be chemically modified by covalent linkage, hydrophobic attraction, silanization, or electrostatic attraction.[1] However, since the emission of II-VI QDs occurs in the visible wavelength range, their use is limited in deep-tissue imaging. This limitation may potentially be overcome by using IV-VI semiconductor nanocrystals, such as PbS QDs, which have tuneable emission in the NIR wavelength region.[4–7] The use of this type of QD for biological applications is still largely unexplored.

This work describes the successful synthesis of an aqueous soluble NIR fluorescent composite based on a PbS QD entrapped in the hollow core of a horse spleen apoferritin (AFt) protein cage by two different approaches, termed reassembly and nanoreactor routes. Of particular interest is the reassembly method, see Figure 1. This involves disassembly of the apoferritin shell into its component protein subunits and then reassembly of the protein shell in the presence of preformed PbS QDs. To our knowledge this method has never previously been used to 'trap' nanocrystals and could be implemented to create other hybrid nanocomposites based on novel preformed and/or commercially available nanocrystals. Most importantly, we demonstrate that the apoferritin-PbS construct provides a stable fluorescent composite in the NIR. This property of the composite combined with its solubility in water and the fact that apoferritin provides an exterior protein coat to the QD that allows covalent attachment of other biomolecules using well-established chemical techniques,[8] may open up novel opportunities in the emerging field of NIR imaging in biology and medicine.

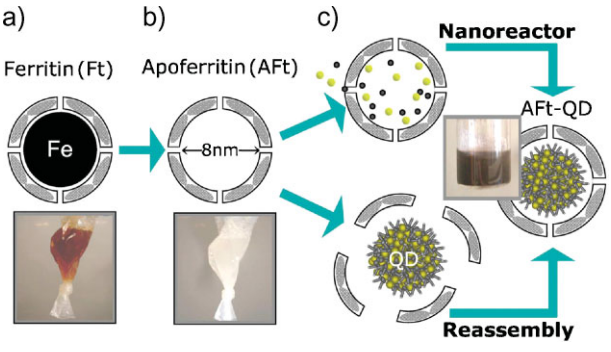

Figure 1. Cartoons of a) ferritin and b) apoferritin. c) Scheme for the synthesis of AFt-PbS composites using the reassembly (bottom) and nanoreactor (top) routes. Photographs in parts (a), (b), and (c) show solutions of Ft, AFt, and AFt-PbS composites.

[*] Prof. N. R. Thomas, B. Hennequin, Dr. L. Turyanska
Centre for Biomolecular Sciences, School of Chemistry
University of Nottingham
Nottingham NG7 2RD (UK)
E-mail: neil.thomas@nottingham.ac.uk
Dr. A. Patanè
School of Physics & Astronomy
University of Nottingham
Nottingham NG7 2RD (UK)
E-mail: amalia.patane@nottingham.ac.uk
Dr. T. Ben, A. M. Beltrán, Prof. S. I. Molina
Departamento de Ciencia de los Materiales e I. M. y Q. I.
Facultad de Ciencias
Universidad de Cádiz
11510 Puerto Real (Spain)
Dr. M. Li, Prof. S. Mann
Centre for Organized Matter Chemistry, School of Chemistry
University of Bristol Bristol
BS8 1TS (UK)

[**] This work is supported by the Medical Research Council, the Engineering and Physical Sciences Research Council, the University of Nottingham, the European Commission (SANDiE Network of Excellence, NMP4-CT-2004-500101), and the Junta de Andalucía (PAI research group TEP-120). The authors thank Prof. Yang Scott, Dr. Adrienne Davis, and Dr. Liu Tong at the University of Nottingham for useful discussions.

We use the iron storage protein ferritin (Ft) as a template for the preparation of the apoferritin-PbS composites. Ferritin molecules are ubiquitous in higher organisms and are used to temporarily store iron ions as their hydrated Fe^{III} oxide so avoiding the toxicity due to free radicals that can be generated with Fe^{III}, which is readily reduced to Fe^{II}.[9] Ferritin consists of a protein shell with an iron oxide core of typically 500–5 000 Fe^{III} atoms as their hydroxide (Fig. 1a). The protein shell, apoferritin (AFt), is composed of 24 subunits of two types 'H'(heavy/heart) and 'L'(light/liver) ($M_w = 22$ kDa and 19 kDa, respectively), which assemble into a hollow protein sphere with outer and inner diameters of 12 nm and 8 nm, respectively (Fig. 1b).[10–12] Apoferritin is also known for its ability to self-assemble: its shell disassembles into subunits at pH < 3.0 and reassembles as an intact sphere at pH > 5.[13] The reassembly route has been used to encapsulate a variety of small organic and inorganic species such as drugs,[14,15] a gadolinium MRI contrast agent,[16] hexacyanoferrate(III),[17] and fluorescein,[18] but has never been exploited for the encapsulation of nanocrystals. However, a variety of apoferritin structures containing metal nanoparticles[19,20] and semiconductor nanocrystals[21–23] have been prepared by an alternative nanoreactor route in which the flow of nanoparticle ion precursors into the hollow core takes place through specific channels at the interface of the apoferritin protein subunits. The large number of aspartate and glutamate residues on the inner surface of the apoferritin shell are thought to promote the formation of the inorganic nanocrystals. Here we exploit both the apoferritin reassembly and nanoreactor properties to synthesize AFt-PbS composites that are not only water-soluble but also optically active in the NIR region.

We have prepared apoferritin from ferritin using a reductive dissolution process established by Mann[24] and modified from that of Granick and Michaelis[11] with dithionite as the reducing agent. The preparation consists of repetitive cycles of a demineralization procedure. The progressive release of iron is clearly seen by a color change of the solution from red-brown for ferritin (Fig. 1a) to pale yellow for the demetallated apoferritin (Fig. 1b). Inductively coupled plasma-mass spectrometry (ICP-MS) analysis indicates that the iron remaining in AFt is about 0.18% of the original value in Ft. This is lower than the residual iron percentage (2%) previously reported by Price and Joshi as determined using thioglycolate.[25]

To form the AFt-PbS composite, we have exploited the two routes shown schematically in Figure 1. For the nanoreactor route, we injected $Pb(AcO)_2$ and Na_2S in deionized water to intact apoferritin cages in 0.1 M NaOAc buffer at pH = 5.5. For the reassembly route, disassembled apoferritin in 0.1 M NaCl was adjusted to pH = 2.0 with 2 M HCl (aq.). This was then added slowly to the preformed thiol-capped PbS quantum dots in deionized water and the pH of the solution was increased to 9.0 to induce reassembly of apoferritin around the dots.

The solutions generated by these routes were examined several times over a period of 3 months by photoluminescence (PL) spectroscopy. For PL experiments, the AFt-PbS composites were studied as liquid solutions in a glass vial or deposited on a glass substrate. The optical excitation was provided by the 514.5 nm line of an Ar^+ laser. The luminescence was dispersed by a 1/2 m monochromator and detected by a cooled (InGa)As photodiode. For atomic force microscopy (AFM) measurements, the PbS QDs and AFt-PbS composites were dispersed onto a polished (100)-oriented p-type Si-substrate. Following the dilution of the solution with deionized water to 1 part in 100, a small drop was then deposited on the substrate and spin-coated for 30 s at a speed of 250 rpm (revolutions per minute). High-resolution transmission electron microscopy (HRTEM) images were recorded on a JEOL2011EX microscope operating at 200 kV. High angle annular dark field scanning transmission electron microscopy (HAADF-STEM) and electron energy loss spectroscopy (EELS) were performed

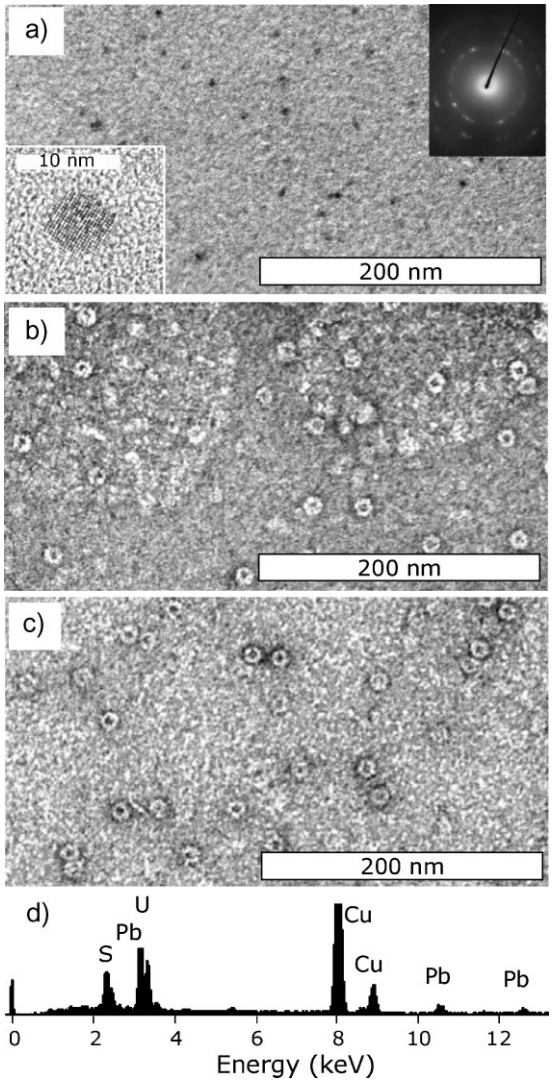

Figure 2. a) TEM image of unstained AFt-PbS composites synthesized using the nanoreactor route. TEM images of AFt-PbS composites stained with uranyl acetate and synthesized using the b) nanoreactor and c) reassembly routes. d) EDX spectra of stained AFt-PbS composites. The U- and Cu- lines arise from the uranyl acetate stain and TEM grid, respectively. The insets in part (a) shows the HRTEM image and XRD pattern for unstained AFt-PbS composites synthesized using the reassembly route.

ADVANCED MATERIALS

with a JEOL 2010F microscope operating at 200 keV and equipped with a GIF camera providing an energy resolution of about 1.6 eV. Energy dispersive X-ray (EDX) spectra were recorded with an Oxford Instruments ultrathin-window EDX detector. Electron microscopy specimens were prepared by depositing the particles to be investigated onto lacey carbon-coated 3 mm copper grids.

Our AFM studies of the PbS QDs[26] indicate that the dots have approximately spherical shape with average height, d, increasing from about 3 to 12 nm for Pb/S molar ratio (MR) increasing from 1:0.2 to 1:0.7. Here we focus on QDs with Pb/S MR = 1:0.3 and average height $d = (5 \pm 2)$ nm.[26] To reveal the morphology and structure of the AFt-PbS composites, we have performed TEM experiments. In Figure 2a, the PbS core of the composite tends to dominate the contrast in the TEM image compared to the rather weaker contrast for the protein shell. The latter can be revealed clearly when the composites are negatively stained with uranyl acetate (Fig. 2b and c). The TEM images of Figure 2b and c show AFt-PbS composites made of an intense central core and a lighter shell. From the analysis of the TEM images of Figure 2b and c, we find that the average diameter of the composite is $d = (13 \pm 1)$ nm, which is consistent with the value expected for apoferritin ($d = 12$ nm). EDX spectra for stained and unstained samples (Fig. 2d) also reveal characteristic Pb- and S-lines thus supporting the presence of a PbS core inside apoferritin. We note that the size indicated by our AFM studies for the AFt-PbS composites ($d = (9 \pm 5)$ nm) and for AFt ($d = (9 \pm 4)$ nm) are smaller than those indicated by TEM. This discrepancy is caused by the compression of the apoferritin shell induced by the AFM-tip, an effect also observed by other groups for ferritin.[27]

To reveal the crystal structure of the core in the AFt-PbS composite, we have examined selected area electron diffraction (SAED) and HRTEM images. The SAED pattern of Figure 2a displays peaks corresponding to interplanar distances of (1.31 ± 0.02) Å and (2.09 ± 0.01) Å, characteristic of the (420) (1.327 Å) and (220) (2.098 Å) planes of bulk PbS.[28] Crystal planes can be also seen in the HRTEM images (Figs. 2a and 3a). Analysis of HRTEM images for several composites (>35) also indicate that the PbS core has an average diameter $d = (6 \pm 2)$ nm. This estimate is close to the size of the PbS QDs without apoferritin derived from both AFM ($d = (5 \pm 2)$ nm)[26] and HRTEM ($d = (6 \pm 2)$ nm) experiments.

As further proof of the incorporation of PbS in apoferritin, we have examined EEL spectra (Fig. 3b) and HAADF images (Fig. 3c) taken with a STEM microscope. This is a well-suited technique to investigate the chemical composition of nanostructures[29,30] and does not require the use of staining agents as the contrast in the image is determined by the atomic number of the constituent elements. Figure 3b shows a sequence of EEL spectra, each taken at a particular position along the line crossing the circular particle marked in the inset of the figure by an arrow. The EEL spectra indicate that the outer layer of the particle contains N-, C-, and S-atoms as expected for the shell of AFt, while a larger number of S-atoms and a significant reduction of C are revealed in the particle core

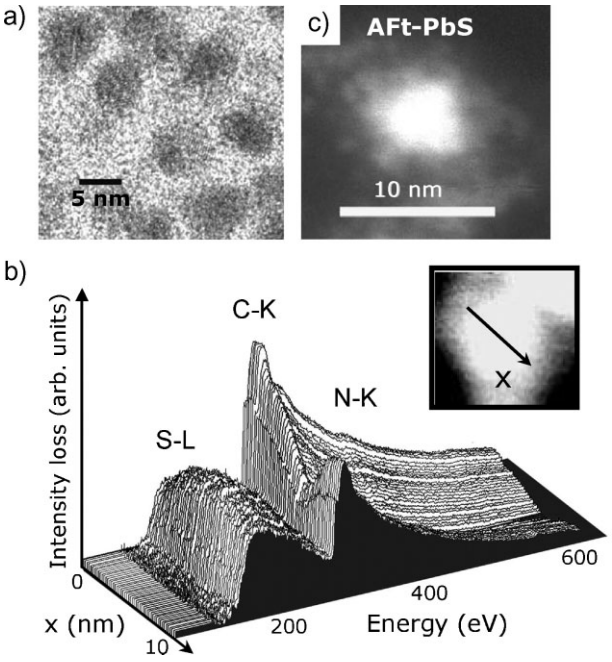

Figure 3. a) HRTEM images and b) spatial sequence of EELS spectra for AFt-PbS composites synthesized using the nanoreactor route. The spectra were recorded with an acquisition time of 1 s and show the characteristic signals of S–L (~165 eV), C–K (~285 eV), and N–K (~401 eV) edges. The inset shows the HAADF image for one composite. Each EEL spectrum was taken at a particular *x*-position along the arrow crossing the composite in the HAADF image. c) STEM-HAADF image of unstained AFt-PbS composites synthesized using the reassembly route.

as expected for PbS. The HAADF-STEM image in Figure 3c also reveals composites made of a lighter shell surrounding a brighter core, which supports the shell–core structure of the AFt-PbS composite.

As shown in Figure 4, the PbS dots and the AFt-PbS composites are both optically active in the NIR spectral region of the electromagnetic spectrum. However note that the encapsulation of the PbS dots in apoferritin tends to shift slightly the PL emission to higher energy values. The small energy shift, ΔE, is similar for the two encapsulation methods and suggests that apoferritin may act to limit the size of the dot it can encapsulate to the size of its core, i.e., $d \sim 8$ nm. In turn this would prevent Ostwald ripening and coalescence of the dots thus preserving smaller dots with correspondingly higher emission energies. The value of ΔE for AFt-PbS solutions based on dots with different emission energies is shown in Figure 4. This shift is also observed when comparing the PL spectra of the different particles resulting from the centrifugation of the AFt-PbS solution. Centrifugation of the AFt-PbS composite solution causes a partial phase separation into a light brown upper solution and a dark brown lower solution (not a solid precipitate) with an ill-defined interface. The AFt-PbS composite, which tends to concentrate in the lower phase, was carefully removed using a syringe and deposited on

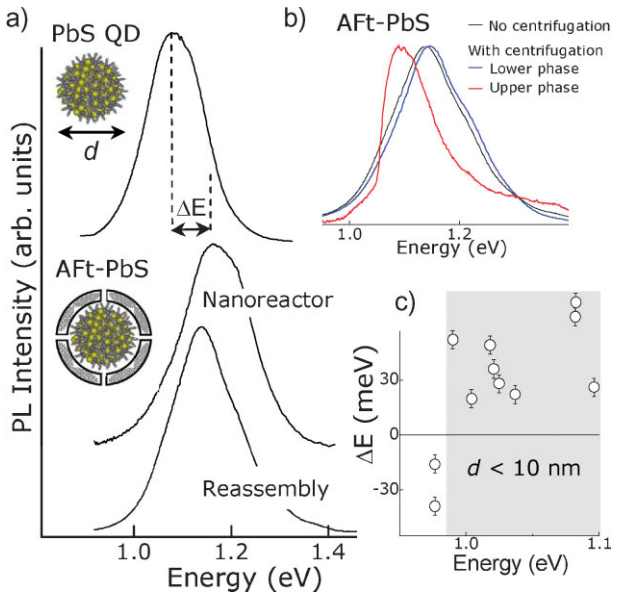

Figure 4. a) Room temperature PL spectra of PbS QDs (Pb/S MR = 1:0.3) and AFt-PbS composites. ΔE is the energy shift of the PL emission of the AFt-PbS solution relative to that of PbS QDs. b) Normalized PL spectra at RT for the AFt-PbS solutions with and without centrifugation. c) Dependence of ΔE on the peak energy of the QD PL emission for dots with different Pb/S MR. The value of ΔE is derived by comparing the PL spectra of PbS QDs and of AFt-PbS composites synthesized using the reassembly route. The grey area indicates dots with average size $d < 10$ nm.

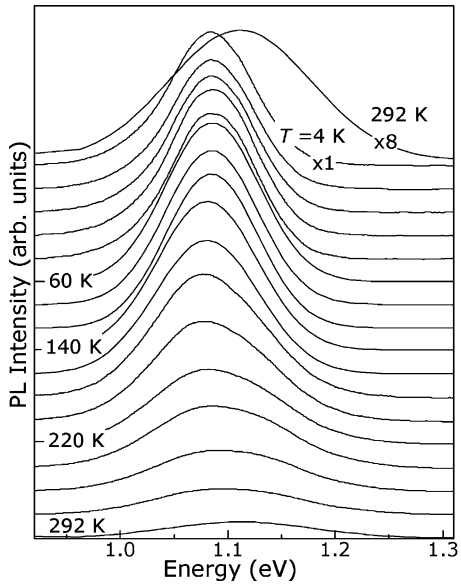

Figure 5. PL spectra of AFt-PbS composites at various T and excitation power $P = 0.2\ \mathrm{Wcm^{-2}}$.

a glass substrate for PL studies. As shown in Figure 4, the emission energy of the lower phase is very similar to that of the original AFt-PbS solution, while that of the upper phase is shifted to lower energy and coincides with that of PbS dots formed in the absence of apoferritin.

The intensities of the PL emissions from the PbS QDs and AFt-PbS composites are comparable and found to be stable over a period of at least 3 months. The stable PL signal of the AFt-PbS composites allowed us to study their optical properties over a wide range of temperatures, T, from 4 K to room temperature, and of excitation powers, P (10^{-3}–10 $\mathrm{Wcm^{-2}}$). For the temperature study, the as-prepared sample was dried on a glass substrate. As shown in Figure 5, with increasing T from 4 to 292 K, the peak energy, E, of the PL spectrum for the AFt-PbS composites blue-shifts and its T-dependence for $T > 150$ K can be described by the coefficient $\alpha = dE/dT = 0.3\ \mathrm{meV\ K^{-1}}$ as expected for PbS QDs.[26] The peak intensity of the PL emission decreases monotonically by less than a factor 10; this high thermal stability of the PL intensity indicates strong carrier confinement in the QD and a relatively low density of nonradiative recombination centres in the AFt-PbS composite.

In conclusion we exploited both the reassembly and nanoreactor properties of apoferritin to incorporate PbS quantum dots in the apoferritin cage. Apoferritin-PbS composites were prepared in aqueous solution and have photoluminescence emission in the wavelength region (~1 μm) of interest for studies of biological media. The apoferritin cages could provide an exterior coat to the quantum dot that is amenable to the attachment of further proteins, saccharides or other biomolecules using standard conjugation chemistry.[8]

Experimental

Preparation of Apoferritin: Apoferritin was prepared using the procedure described in reference [24]. The native horse spleen ferritin protein (255 mg, 0.34 mmol) diluted in 27 mL 0.1 M NaOAc buffer (pH 5.5) was first dialyzed against NaOAc buffer (0.1 M, 820 mL) at pH 5.5 for 20 min; mercaptoacetic acid (2 mL, 0.03 M) was then added to the buffer and dialyzed for 2 h against 0.1 M NaOAc pH 5.5 (820 mL); further mercaptoacetic acid (1 mL, 0.03 M) was added and dialysis continued for an additional hour against 0.1 M NaOAc pH 5.5 (820 mL); finally, the buffer was refreshed for 20 min. This process was repeated until reaching a complete decoloration of the ferritin solution.

Synthesis of PbS QDs: To synthesize PbS QDs, we prepared a 60 mL solution containing lead acetate trihydrate $Pb(AcO)_2 \cdot 3H_2O$ (0.364 g, 0.96 mmol) and a mixture of thiols, i.e., thioglycerol (TGL) (0.52 mL, 0.006 mol) and dithioglycerol (DTG) (0.20 mL, 0.002 mol), which act as capping agents. The synthesis of the dots was completed by adding a 0.1 M solution of sodium sulphide Na_2S (0.25 mL to 0.58 mL for Pb/S MR varying from 1:0.3 to 1:0.7) forming dots of diameter d in the range 3 to 12 nm.

Synthesis of AFt-PbS Composites: For the nanoreactor route, we injected $Pb(AcO)_2$ (5 mL, 0.08 mol) and 0.1 M Na_2S (0.25 mL to 0.58 mL for Pb/S molar ratio (MR) varying from 1:0.3 to 1:0.7) to apoferritin (5 mL, 0.09 mmol) at pH = 5.5 under vigorous stirring. The resulting solution was mixed for 15 min after the injection. For the reassembly route, the pH (=11) of a 5 mL solution of preformed PbS QDs was adjusted to 9.5 by adding 0.1 M HCl. Apoferritin (5 mL, 0.09 mmol) was adjusted to pH = 2.0 by dialysis against a 0.1 M NaCl solution (150 mL), whose pH was controlled by HCl. Then disassembled apoferritin was added slowly to the preformed quantum dots. Both syntheses were

ADVANCED MATERIALS

carried out under a N_2 atmosphere. The solutions were stored in a fridge at a temperature of 278 K under a N_2 atmosphere. For the centrifugation experiment, the AFt-PbS solutions were centrifuged at 402× *g* for 5 min at 16 °C using a S4180 rotor in a Beckman GS-15R centrifuge.

Received: February 25, 2008
Revised: April 23, 2008
Published online: September 1, 2008

[1] X. Michalet, F. F. Pinaud, L. A. Bentolila, J. M. Tsay, S. Doose, J. J. Li, G. Sundaresan, A. M. Wu, S. S. Gambhir, S. Weiss, *Science* **2005**, *307*, 538.
[2] C. R. Simpson, M. Kohl, M. Essenpreis, M. Cope, *Phys. Med. Biol.* **1998**, *43*, 2465.
[3] T. Pellegrino, S. Kudera, T. Liedl, A. Muñoz Javier, L. Manna, W. J. Parak, *Small* **2005**, *1*, 48.
[4] L. Bakueva, I. Gorelikov, S. Musikhin, X. S. Zhao, E. H. H. Sargent, E. Kumacheva, *Adv. Mater.* **2004**, *16*, 926.
[5] L. Levina, V. Sukhovatkin, S. Musikhin, S. Cauchi, R. Nisman, D. P. Bazett-Jones, E. H. Sargent, *Adv. Mater.* **2005**, *17*, 1854.
[6] J. H. Choi, K. H. Chen, M. S. Strano, *J. Am. Chem. Soc.* **2006**, *128*, 15584.
[7] B. R. Hyun, H. Chen, D. A. Rey, F. W. Wise, C. A. Batt, *J. Phys. Chem. B* **2007**, *111*, 5726.
[8] G. T. Hermanson, *Bioconjugate Techniques*, Academic, New York **1996**.
[9] R. R. Crichton, *FEBS Lett.* **1973**, *34*, 125.
[10] S. Granick, *J. Biol. Chem.* **1942**, *146*, 451.
[11] S. Granick, L. Michaelis, *J. Biol. Chem.* **1943**, *147*, 91.
[12] E. C. Theil, *Annu. Rev. Biochem.* **1987**, *56*, 289.
[13] P. M. Harrison, D. W. Gregory, *Nature* **1968**, *220*, 578.
[14] J. M. Domínguez-Vera, *J. Inorg. Biochem.* **2004**, *98*, 469.
[15] Z. Yang, X. Wang, H. Diao, J. Zhang, H. Li, H. Sun, Z. Guo, *Chem. Commun.* **2007**, *3453*.
[16] S. Aime, L. Frullano, S. Geninatti Crich, *Angew. Chem. Int. Ed.* **2002**, *41*, 1017.
[17] J. M. Domínguez-Vera, E. Colacio, *Inorg. Chem.* **2003**, *42*, 6983.
[18] G. Liu, J. Wang, S. A. Lea, Y. Lin, *Chem. Bio. Chem.* **2006**, *7*, 1315.
[19] M. Li, C. Viravaidya, S. Mann, *Small* **2007**, *3*, 1477.
[20] N. Gálvez, P. Sánchez, J. M. Domínguez-Vera, A. Soriano-Portillo, M. Clemente-León, E. Coronado, *J. Mater. Chem.* **2006**, *16*, 2757.
[21] K. K. W. Wong, S. Mann, *Adv. Mater.* **1996**, *8*, 928.
[22] I. Yamashita, J. Hayashi, M. Hara, *Chem. Lett.* **2004**, *1158*.
[23] K. Iwahori, K. Yoshizawa, M. Muraoka, I. Yamashita, *Inorg. Chem.* **2005**, *44*, 6393.
[24] K. K. Wong, H. Cölfen, N. T. Whilton, T. Douglas, S. Mann, *J. Inorg. Biochem.* **1999**, *76*, 187.
[25] D. J. Price, J. G. Joshi, *J. Biol. Chem.* **1983**, *258*, 10873.
[26] L. Turyanska, A. Patanè, M. Henini, B. Hennequin, N. R. Thomas, *Appl. Phys. Lett.* **2007**, *90*, 101913.
[27] D. N. Axford, J. J. Davis, *Nanotechnology* **2007**, *18*, 145502.
[28] M. Flores-Acosta, M. Sotelo-Lerma, H. Arizpe-Chávez, F. F. Castillón-Barraza, R. Ramírez-Bon, *Solid State Commun.* **2003**, *128*, 407.
[29] O. Stephan, P. M. Ajayan, C. Colliex, P. Redlich, J. M. Lambert, P. Bernier, P. Lefin, *Science* **1994**, *266*, 1683.
[30] K. Suenaga, M. Tencé, C. Mory, C. Colliex, H. Kato, T. Okazaki, H. Shinohara, K. Hirahara, S. Bandow, S. Iijima, *Science* **2000**, *290*, 2280.